Smart Structures and Systems, *Vol. 15, No. 3 (2015) 645-663*
DOI: http://dx.doi.org/10.12989/sss.2015.15.3.645

Displacement estimation of bridge structures using data fusion of acceleration and strain measurement incorporating finite element model

Soojin Cho, Chung-Bang Yun and Sung-Han Sim*

School of Urban and Environmental Engineering, Ulsan National Institute of Science and Technology (UNIST), Ulsan 689-798, Republic of Korea

(Received November 5, 2014, Revised February 10, 2014, Accepted February 12, 2015)

Abstract. Recently, an indirect displacement estimation method using data fusion of acceleration and strain (i.e., acceleration-strain-based method) has been developed. Though the method showed good performance on beam-like structures, it has inherent limitation in applying to more general types of bridges that may have complex shapes, because it uses assumed analytical (sinusoidal) mode shapes to map the measured strain into displacement. This paper proposes an improved displacement estimation method that can be applied to more general types of bridges by building the mapping using the finite element model of the structure rather than using the assumed sinusoidal mode shapes. The performance of the proposed method is evaluated by numerical simulations on a deck arch bridge model and a three-span truss bridge model whose mode shapes are difficult to express as analytical functions. The displacements are estimated by acceleration-based method, strain-based method, acceleration-strain-based method, and the improved method. Then the results are compared with the exact displacement. An experimental validation is also carried out on a prestressed concrete girder bridge. The proposed method is found to provide the best estimate for dynamic displacements in the comparison, showing good agreement with the measurements as well.

Keywords: Displacement; bridge; data fusion; finite element model; modal mapping

1. Introduction

Displacement is an intuitive response that directly results from external loads to a structure. Despite of its close relationship with health of a structure, displacement has not been popularly used in structural health monitoring (SHM) of full-scale civil engineering structures unlike other responses such as acceleration (Doebling *et al*. 1998, Bani-Hani *et al*. 2008, Altunisik *et al*. 2012) and strain (Omenzetter *et al*. 2004, Majumder *et al*. 2008, Sigurdardottir and Glisic 2014); a limited number of literatures have reported the use of displacement for monitoring of civil structures (Faulkner *et al*. 1996, Celibi 2000, Xu *et al*. 2002, Nassif *et al*. 2005, Lee *et al*. 2007). The literatures, however, exhibit that the usage is limited to the measurements at a few locations, which is incapable of providing rich information necessary to assess comprehensive structural

*Corresponding author, Assistant Professor, E-mail: ssim@unist.ac.kr

http://www.techno-press.org/?journal=sss&subpage=8 ISSN: 1738-1584 (Print), 1738-1991 (Online)

health.

The usage of displacement has been restricted in full-scale civil structures due to measurement inconvenience and high cost of measurement devices. The traditional contact-type transducers, such as a linear variable differential transformer (LVDT) and a ring type transducer, measure displacements from the deformation of an elastic part of the transducer that is contacted to the structure. The contact-type transducers are inexpensive, but require reference points to fix the transducer firmly when the host structure is deforming. In many cases, some fixtures such as scaffolds are installed around the structure to bind the transducers, which is labor intensive and often unavailable due to operational condition of the structure. Even the fixtures may be deformed by an external force such as wind. Noncontact-type devices, such as the global positioning system (GPS) and the laser Doppler vibrometer (LDV), have been emerged as alternatives (Nassif *et al*. 2005, Jo *et al*. 2013). However, high cost of the devices up to a few ten thousand dollars per sensing channel still limits their real-world applications with a dense topology.

To overcome the inherent limitations of displacement transducers, indirect displacement estimation approaches have alternatively been studied to use other responses that can be converted to the displacement. Acceleration and strain are the most popular responses in the studies. Acceleration is an absolute response that can be easily captured on a structure without having a fixed reference. Theoretically, acceleration can be converted into displacement by double integration in the time domain, while the numerical integration generally brings a significant signal drift (Park *et al*. 2005, Gindy *et al*. 2008, Kandula *et al*. 2012). Lee *et al*. (2010) successfully proposed an FIR filter-based displacement estimation technique which regularizes the signal drift. However, the acceleration-displacement conversion is based on the low-pass filter that eliminates the signal drift with true low frequency component contained in the displacement signal. Thus, the acceleration-based technique fails to estimate displacement with the static or pseudo-static components. Unlike the acceleration, strain can estimate the static or pseudo-static displacement in nature as the time integration is uninvolved in the conversion. Displacement may be estimated from strain using double spatial integration in space when the strain is measured on a structure in the distributed manner (Chung *et al*. 2008) or using the modal mapping between a strain and displacement (Foss and Hauge 1995). Since the modal mapping may construct dynamic displacement from a few measured dynamic strain data based on the modal information, it is very useful to estimate displacements at arbitrary locations on the structure when its modal information is available. Instead of using modal information measured by densely deployed sensors, Kang *et al*. (2007) used mode shapes from the finite element (FE) model of a structure and Shin *et al*. (2012) used assumed sinusoidal mode shapes for a simple beam-type structure. The strain does not cause the signal drift in time domain during the conversion to displacement, while its measurement is vulnerable to measurement noise in high frequency range. Furthermore, the strain-based method requires determination of neutral axis of the structure (Shin *et al*. 2012).

Park *et al*. (2013) proposed a displacement estimation method using data fusion of acceleration and strain by extending the acceleration-based method proposed by Lee *et al*. (2010). In the regularization term, the displacement converted from strain data by the modal mapping is used to prevent the signal drift. For the modal mapping, the assumed analytical (sinusoidal) mode shapes proposed by Shin *et al*. (2012) are employed. The method by Park *et al*. (2013), however, inherits a limitation in application to more general types of bridges with complex shapes, such as arch and truss bridges, since the method uses assumed sinusoidal mode shapes which may be reasonably obtained only for the girder bridges.

This study proposes an improved method to estimate the accurate displacement using

acceleration and strain for general bridge structures. The proposed method is to extend the method by Park *et al*. (2013) to general types of bridges by using the mode shapes for the modal mapping from the FE model of a structure instead of assumed sinusoidal mode shapes. The performance of the proposed method is evaluated by numerical simulations on a deck arch bridge model and a three-span truss bridge model whose mode shapes are hard to be assumed as sinusoidal functions. The displacements are estimated by acceleration-based method, strain-based method, fusion-based method, and the improved method, and the results are compared with exact displacements to demonstrate the performance of the proposed method. Then, the method is experimentally validated from a field testing on a prestressed concrete bridge. From the comparison of displacements estimated by the four methods to the reference values measured by laser displacement meters, the accuracy of the proposed method has been investigated. The proposed method makes the displacement measurement facilitated (without the reference points), inexpensive, and accurate.

2. Improved displacement estimation method using acceleration and strain

This section describes the principles of the displacement estimation method proposed by Park *et al*. (2013) and the modification made in the proposed method.

2.1 Acceleration-strain-based displacement estimation method

Park *et al*. (2013) have proposed the displacement estimation method by fusing the acceleration and strain. The method uses the basic form of the acceleration-based method proposed by Lee *et al*. (2010), while the regularization term is replaced by the difference between estimated displacements and displacement estimated from the strain by modal mapping method. The method can be formulated for displacement $\mathbf{u}_i$ at the location of x_i as

$$\underset{\mathbf{u}_i}{\text{Min}}\,\Pi = \frac{1}{2}\left\|\mathbf{L}_a(\mathbf{L}_c\mathbf{u}_i - (\Delta t)^2\bar{\mathbf{a}}_i)\right\|_2^2 + \frac{\lambda^2}{2}\left\|\mathbf{u}_i - \bar{\boldsymbol{\varepsilon}}\mathbf{D}_i^{\mathrm{T}}\right\|_2^2 \tag{1}$$

where $\mathbf{u}_i \in ¡^{(N+2)\times 1}$ and $\bar{\mathbf{a}}_i \in ¡^{N\times 1}$ are the estimated displacement and measured acceleration at the location x_i; $\bar{\boldsymbol{\varepsilon}} \in ¡^{(N+2)\times n}$ is the strain measured at n locations; N is the number of acceleration data to be converted into displacement; Δt is the time step; $\mathbf{L}_a \in ¡^{N\times N}$ is a diagonal weighting matrix having the first and last entries as $1/\sqrt{2}$ and the other entries as 1; $\mathbf{L}_c \in ¡^{N\times(N+2)}$ is the second-order differential operator matrix of the discretized trapezoidal rule (Atkinson 2008); $\|\cdot\|_2$ is2-norm of a vector; λ is a regularization factor; and $\mathbf{D}_i \in ¡^{1\times n}$ is the ith row of modal mapping matrix $\mathbf{D} \in ¡^{m\times n}$ that converts strain into displacement as

$$\mathbf{u}^{\mathrm{T}} = \mathbf{D}\bar{\boldsymbol{\varepsilon}}^{\mathrm{T}} \tag{2}$$

where $\mathbf{u} \in ¡^{(N+2)\times m}$ is the displacement obtained at m locations. The modal mapping matrix can be calculated as

$$\mathbf{D} = \boldsymbol{\Phi}\boldsymbol{\Psi}^{\dagger} \tag{3}$$

where $\mathbf{\Phi} \in ¡^{m \times r}$ and $\mathbf{\Psi} \in ¡^{n \times r}$ denote mode shape vector and strain mode shapes, respectively; the superscript † denotes the pseudo-inverse; and r is the number of used modes that is equal to or smaller than n to avoid an under-determined modal mapping matrix. Note that the number of modes n used in the estimation can be determined based on dominant modes in the displacement being estimated. λ is defined by Lee *et al*. (2010) as

$$\lambda = 46.81N^{-1.95} \tag{4}$$

The mode shapes and strain mode shapes may be directly estimated from measurements, which would be very expensive. Instead, Park *et al*. (2013) employed assumed sinusoidal mode shapes and corresponding strain mode shapes, proposed by Shin *et al*. (2012), as

$$\mathbf{\Phi}^{assumed} = \begin{bmatrix} \sin\frac{\pi x_1}{l} & \mathrm{L} & \sin\frac{r\pi x_1}{l} \\ \mathrm{M} & \mathrm{O} & \mathrm{M} \\ \sin\frac{\pi x_m}{l} & \mathrm{L} & \sin\frac{r\pi x_m}{l} \end{bmatrix} \tag{5}$$

$$\mathbf{\Psi}^{assumed} = \frac{y\pi^2}{l^2}\begin{bmatrix} \sin\frac{\pi z_1}{l} & \mathrm{L} & r^2\sin\frac{r\pi z_1}{l} \\ \mathrm{M} & \mathrm{O} & \mathrm{M} \\ \sin\frac{\pi z_n}{l} & \mathrm{L} & r^2\sin\frac{r\pi z_n}{l} \end{bmatrix} \tag{6}$$

where x_i $(i = 1, \mathrm{L}, m)$ and z_i $(i = 1, \mathrm{L}, n)$ are the locations where acceleration and strain are measured, respectively; y is the distance from the neutral axis to the surface where strain gauges are installed; and l is length of the structure. The neutral axis y can be determined by the calibration technique that uses both acceleration and strain, which was proposed by Park *et al*. (2013). The solution of Eq. (1) can be expressed as

$$\mathbf{u}_i = (\mathbf{L}^T\mathbf{L} + \lambda^2\mathbf{I})^{-1}(\mathbf{L}^T\mathbf{L}_a\bar{\mathbf{a}}_i\Delta t^2 + \lambda^2\bar{\boldsymbol{\varepsilon}}\mathbf{D}_i^{\mathrm{T}}) \tag{7}$$

where $\mathbf{L} = \mathbf{L}_a\mathbf{L}_c$. Note that Lee *et al*. (2010) suggested a moving-window strategy to address the inaccurate estimation near the boundaries of the finite data, which was also adapted by Park *et al*. (2013). The optimal size of moving window is proposed as three times the number of data points in the first natural period after numerical simulation tests on various systems in Lee *et al*. (2010).

2.2 Improved method using modal mapping from finite element model

The acceleration-strain-based method (described in the previous section) builds the modal mapping matrix $\mathbf{D}$ using the assumed sinusoidal mode shapes as in Eqs. (5) and (6). In the case of prismatic or nearly-prismatic simply-supported beams, the sinusoidal mode shapes approximate the real ones reasonably. For example, Shin *et al*. (2012) successfully estimated displacement from the measured strain on a single-span bridge using the assumed sinusoidal mode shapes. Park *et al*. (2013) also validated their method on a suspension bridge in the experiment. Both bridges have

prismatic or nearly-prismatic sections and large span-to-depth ratios, and thus have the mode shapes quite close to the assumed sinusoidal shapes.

However, possible disagreements of the assumed mode shapes to the real mode shapes can happen in general types of structures, causing significant errors in the displacement estimation. The errors can be minimized by obtaining the real mode shapes and strain mode shapes from a dense array of accelerometers and strain gages, but it is not practical due to high cost. If the mode shapes and strain mode shapes can be assumed reasonably based on the physical insight of the structure, then they can minimize the error up to the acceptable level.

In this paper, an improved method is proposed by employing a modal mapping matrix derived from an FE model of the structure as

$$\mathbf{D} = \mathbf{\Phi}^{FE} (\mathbf{\Psi}^{FE})^{\dagger} \tag{8}$$

where $\mathbf{\Phi}^{FE} \in ¡^{m \times r}$ and $\mathbf{\Psi}^{FE} \in ¡^{n \times r}$ are the mode shapes and the strain mode shapes obtained from the FE model. Since $\mathbf{\Phi}^{FE}$ and $\mathbf{\Psi}^{FE}$ replace $\mathbf{\Phi}$ and $\mathbf{\Psi}$ of Eqs. (5) and (6) in the improved method, the mode shapes and the strain mode shapes need to be estimated from the FE model for locations where the displacement is to be estimated (i.e., the accelerations are measured) and where the strains are measured, respectively.

The accuracy of the estimated displacement can be quantified by employing a percentage root mean square deviation (RMSD) as

$$RMSD\ (\%) = \frac{\sqrt{\sum_{j=1}^{N} (u_{ij}^{est} - u_{ij}^{ref})^2}}{\sqrt{\sum_{j=1}^{N} (u_{ij}^{ref})^2}} \times 100 \tag{9}$$

where u_{ij}^{est} and u_{ij}^{ref} are the estimated and reference displacements at location x_i, respectively.

3. Numerical validation

The improved method is validated from numerical simulations carried out on two example structures: an open-spandrel deck arch bridge model and a 3-span truss bridge model. The displacements excited by a moving load are estimated by four methods: i.e., acceleration-based method (Lee *et al*. 2010), strain-based method (Kang *et al*. 2007), acceleration-strain-based method (Park *et al*. 2013), and the improved acceleration-strain-based method, and the results are compared for the validation.

3.1 Deck arch bridge model

The first example used in this study is a 2D open-spandrel deck arch bridge model shown in Fig. 1. The model has a deck which locates above the arch and the deck is supported by a number of vertical columns rising from the arch. The Rainbow Bridge at Niagara Falls and the Cold Spring Canyon Arch Bridge are the famous examples of the deck arch bridges.

The model is composed of 34 members: 12 deck members, 12 arch members, and 10 vertical columns. All members are modelled as frame elements. N# and A# denote the nodes and supports,

respectively. The span length of the bridge is 120 m, and the height of the arch is 20 m. The sectional properties of members for deck, arch, and vertical columns are shown in Table 1.

The displacement, acceleration, and strain of the beam are simulated using MATLAB Simulink. A vertical load moving from left to right of the deck with a constant speed (v =10 m/s), shown in Fig. 2, is employed to generate non-zero mean displacements. The load is the combination of a moving static load of 43.2 ton (DB24 truck load specified in Korean highway bridge design code) and zero-mean Gaussian random load with a standard deviation of 13 ton simulating dynamic loading effect. Acceleration is assumed to be measured at N6, while strains on the deck are obtained at the mid spans of four deck members between N1-N2, N4-N5, N7-N8, and N10-N11. The simulated acceleration and strains are made artificially contaminated by adding 5% noise in root mean square (RMS) to emulate the practical measurement. The displacement simulated at N6 is used as the reference to evaluate the accuracy of estimated displacements. Note that acceleration and displacement are obtained in the vertical direction, while the strains are obtained on the bottom surfaces of the deck in the longitudinal direction to capture the bending strain.

Since four strain data are available in this example, the first four modes are employed to build the modal mapping relationship. Fig. 3 shows the first four mode shapes of the FE model, compared with the sinusoidal shapes based on the assumption of a simply supported prismatic beam. The visual comparison clearly shows the difference between the two types of mode shapes, particularly for the first and third mode shapes near the supports. Their modal assurance criterion (MAC) values are 0.718, 0.936, 0.651, and 0.988, respectively. Thus, it can be expected that the displacement estimated near the supports may have considerable error when the assumed modes are used.

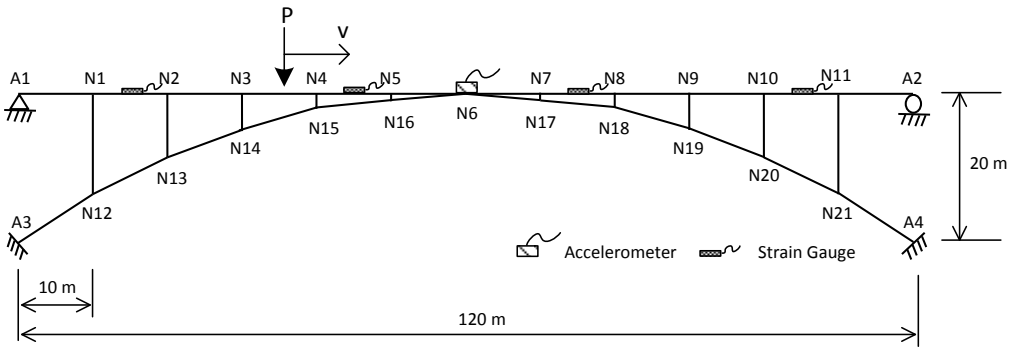

Fig. 1 Deck arch bridge model with sensor topology

Table 1 Structural properties of deck arch bridge model

Members	Deck	Arch	Vertical Column
Sectional area	0.656 m^2	0.280 m^2	0.167 m^2
2nd moment of inertia	1.453×10^{-1} m^4	3.087×10^{-1} m^4	6.535×10^{-2} m^4
Elastic modulus		200 GPa	
Mass density		7850 kg/m^3	

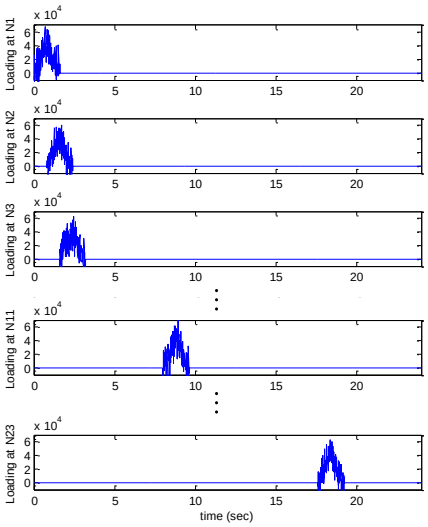

Fig. 2 Simulated vertical moving load

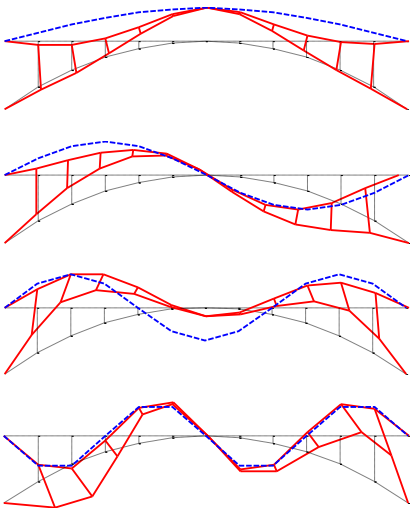

Fig. 3 First four mode shapes of FE model (solid lines) compared with assumed ones (dashed lines)

3.1.1 Comparison of displacements at N6

Fig. 4 shows the comparison of the displacements estimated by four methods with exact one simulated from the MATLAB Simulink. The acceleration-based method can not estimate the nonzero-mean pseudo-static displacement component as shown in Fig. 4(a). The strain-based method can somewhat estimate the static component as shown in Fig. 4(b), while the dynamic component cannot be estimated accurately. The acceleration-strain-based method gives an incorrect displacement due to the incorrect modal mapping as in Fig. 4(c). Meanwhile, the improved acceleration-strain-based method estimates very accurate displacement overlapped with

the exact one as in Fig. 4(d), despite of the complexity of the deck arch model. This clarifies the performance of the improved method for a complex structure whose mode shapes may not be easily assumed as analytical functions.

The accuracy of the estimated displacements can be investigated in the different aspects by looking at the frequency domain. Fig. 5 shows the power spectral density (PSD) of the estimated displacements compared with that of exact one. Figs. 5(a) and 5(b) show errors of the acceleration-based and the strain-based methods in low and high frequency range, respectively. The acceleration-strain-based method shows slightly larger error in estimating the pseudo-static components near 0 Hz than the improved method (see zoomed-ins of Figs. 5(c) and 5(d)).

The peak at 15.4 Hz shown in the PSD of the strain-based method shows a drawback of the strain-based method. The bridge model has a mode at 15.4 Hz, and the corresponding mode shape has a nodal point at N6. This is why there is no peak observed at 15.4 Hz in Fig. 5(a). However, the strains used in the strain-based method were obtained from non-nodal points, and thus the peak is clearly observed. In the acceleration-strain-based and improved methods, the high frequency components contained in the strain were replaced by the components contained in the acceleration, which resulted in the disappearance of the peak at 15.4 Hz in Figs. 5(c) and 5(d). This illustrates that the strain-based method is only effective in estimating the very low-frequency components which have few nodal points.

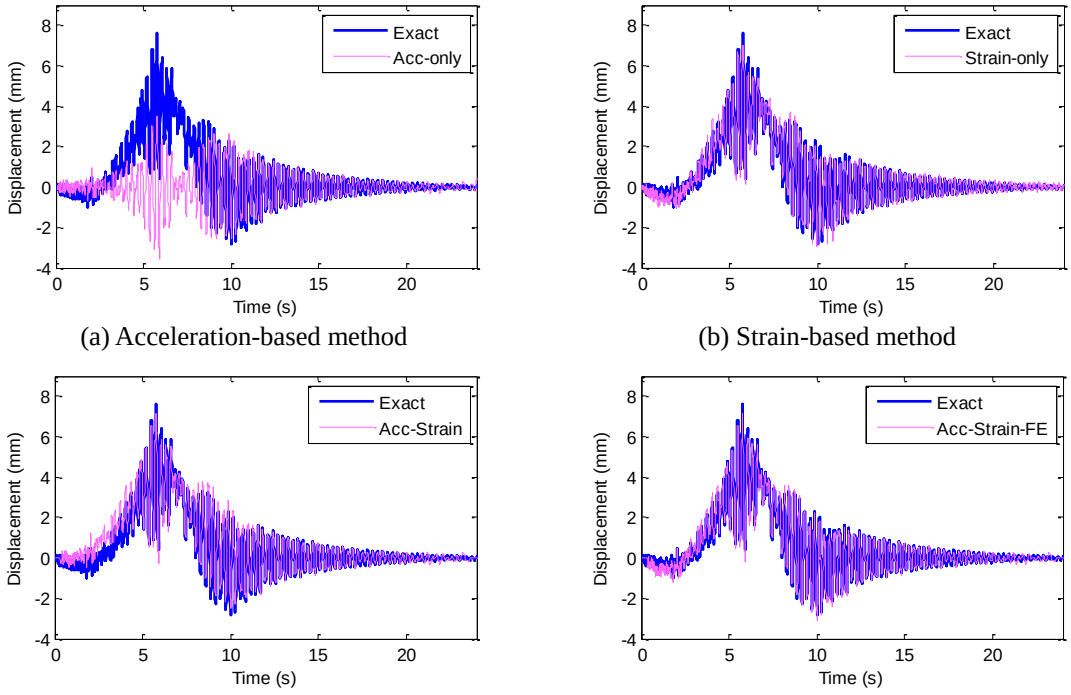

(a) Acceleration-based method

(b) Strain-based method

(c) Acceleration-strain-based method

(d) Improved acceleration-strain-based method

Fig. 4 Comparison of displacements estimated at N6 for deck arch bridge model by four different estimation methods with exact one

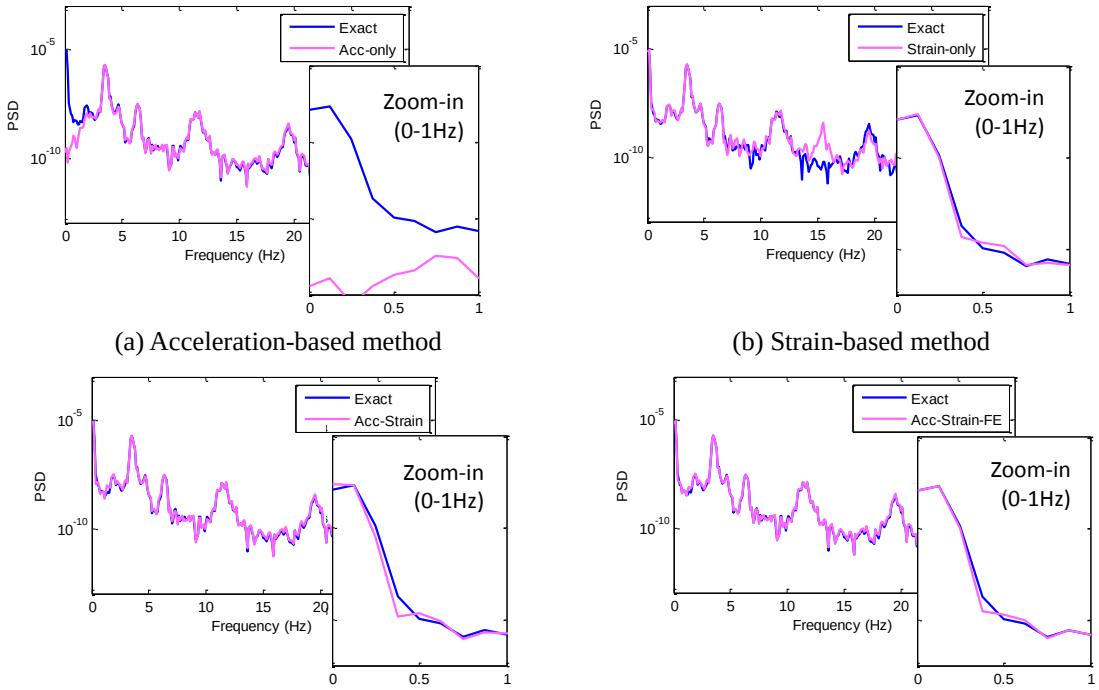

(a) Acceleration-based method (b) Strain-based method

(c) Acceleration-strain-based method (d) Improved acceleration-strain-based method

Fig. 5 Comparison of PSD of displacements estimated at N6 for deck arch model by four different estimation methods with exact one

The accuracy of the estimated displacements by the four methods is quantified using the percentage RMSD described in Eq. (12). The acceleration-based method provides the largest RMSD of 85.9% at N6. The strain-based method yields small error of 17.7%, since the method uses accurate modal mapping using the FE mode shapes. The acceleration-strain-based method gives a larger RMSD value of 20.5% than the strain-based method, which means the error in the assumed mode shapes may bring significant error in the estimation due to incorrect modal mapping. The improved method has the smallest RMSD value of 10.6% owing to accurate modal mapping using the FE model. The estimated RMSD values quantitatively show the performance of the improved method compared with the other existing methods for the general types of bridge structures.

3.1.2 Comparison of displacements at other locations

Fig. 6 shows the RMSD values of the displacements estimated by four methods at the left half of the deck: N1-N6. The acceleration-based method shows largest error for all locations due to incorrect estimation of pseudo-static displacements. The incorrect modal mapping significantly increases the error of the acceleration-strain-based method, which is even larger than the strain-based method that uses correct modal mapping. The improved method has the smallest RMSD values for all points.

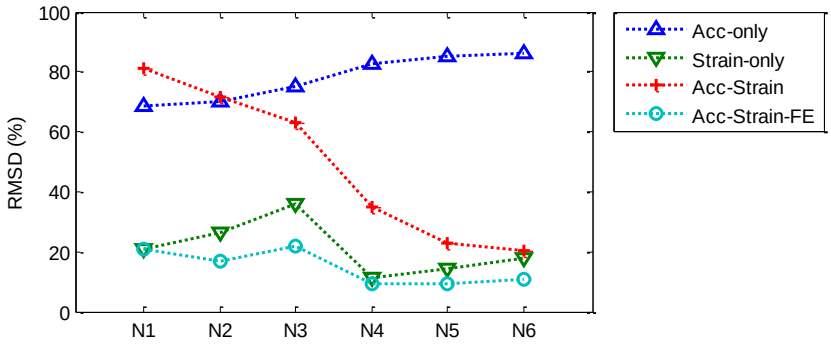

Fig. 6 RMSD of displacements at N1-N6

3.1.3 Effect of FE model inaccuracy

The FE model may be subjected to modelling errors, which may cause estimation errors in the modal properties. To see the effect of the inaccurate FE model to the estimation, the FE model is perturbed by introducing element-level errors in the elastic modulus. Three types of perturbations with 11.5, 23.1, and 34.6% in RMS (i.e., uniform perturbation in the range of ±20%, ±40%, and ±60% of the initial value) are considered. Fig. 7 shows the first four mode shapes of a perturbed FE model with 34.6% errors in RMS in comparison with those from the original FE model. Fig. 7 shows that the perturbation caused considerable discrepancy particularly on the higher mode shapes to be used for the modal mapping.

Fig. 8 shows the RMSDs of the estimated displacements at N6 by the strain-based and the improved methods when the perturbed FE models are used for the modal mapping. The MAC values of the perturbed models are plotted together to show the effect of perturbation to the mode shapes. By the incremental perturbation, the mode shapes are found to change incrementally. However, even with the significant perturbation, the RMSD of the estimated displacement rarely changes for both the strain-based and the improved methods. In the case of with perturbation of 34.6% in RMS, the RMSD by the improved method is 10.8%, which is much smaller than 20.5% by the acceleration-strain-based method in Section 3.1.1. When the exact FE model was used, the RMSDs are 10.6 and 17.7% for the stain-based and the improved methods, respectively. The slight increase by the large perturbation is because the RMS is significantly affected by accuracy of the low frequency components, as shown in the result of the acceleration-based method. The MAC values of Fig. 8 shows that the large perturbation makes bigger change as the mode order increases, and the first mode which significantly affects the RMSDs is barely changed. The inaccuracy in higher modes resulted in inaccurate estimation of dynamic displacements that derives the slight increase of the RMSDs. This illustrates the improved method using the mode shapes of the FE model is very effective when the structure is so complex that its lower mode shapes cannot be easily assumed.

3.1.4 Measurement of strains at load carrying members

In the case of the deck arch bridge, the arch and vertical columns are the major load carrying members to resist the dead loads that comprise majority of the total load applied to the structure, while the deck is designed to transfer the live load to the arch system. Considering the case with strain gauges on the members other than deck, another sensor topology is considered: an

accelerometer is at N6, and four strain gauges are at arch members between N12-N13 and N20-N21, and columns between N3-N14 and N9-N19. Fig. 9 shows the displacement estimated at N6 using the improved method. The result is very close to the exact one with 9.69% in RMSD, which is smaller than the value of 10.6% by the strain measurements on the deck described in Section 3.1.1.

The mode shapes cannot be assumed in an analytical form for the whole structure when the structure has a complex shape. Therefore, the acceleration-strain-based method using the assumed sinusoidal mode shapes is applicable only when the strain gauges are on the deck. This example shows that the proposed improved method based on the FE model has big advantage when the strain sensors are placed on non-deck members.

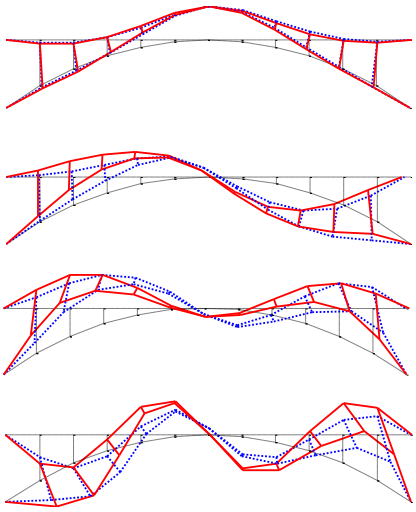

Fig. 7 First four mode shapes of perturbed FE model with 34.6% errors in RMS (dotted lines) compared with those from original model (solid lines)

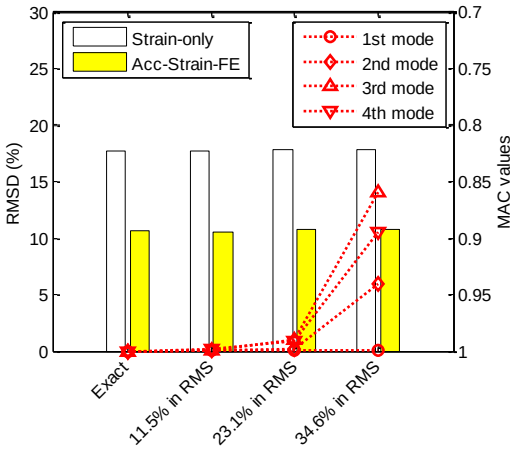

Fig. 8 RMSD of displacements estimated at N5 for perturbed deck arch FE models

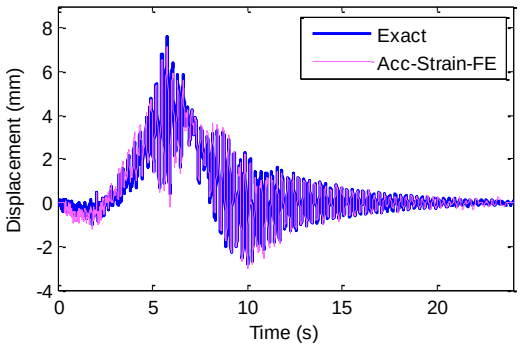

Fig. 9 Displacement estimated at N6 by improved acceleration-strain-based method using strain measurement on load carrying members

3.2 A three-span truss bridge model

The second example is a 2D 3-span truss structure shown in Fig. 10. It is a double-Warren truss model which has intersecting diagonal members to provide the model strength. The model has a total length of 192 m (=56 m+80 m+56 m) with varying heights of 10-18 m. The second support, named A2, is pinned, while the other three supports (A1, A3, and A4) are rollers.

The model is composed of 175 members: 24 lower chords, 24 upper chords, 27 vertical members, and 100 diagonal members. The second span is considered as the monitored span for comparison with acceleration-stain-based method. All members are designed to be made of steel, and to have different sectional areas as shown in Table 2.

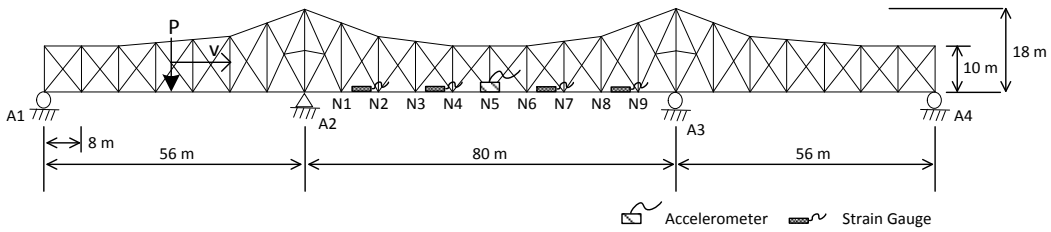

Fig. 10 Three-span truss bridge model with sensor topology

Table 2 Structural properties of truss bridge model

Members	Lower and Upper Chord	Vertical Member	Diagonal Member
Sectional area	0.760 m^2	0.280 m^2	0.360 m^2
Elastic modulus		200 GPa	
Mass density		7850 kg/m^3	

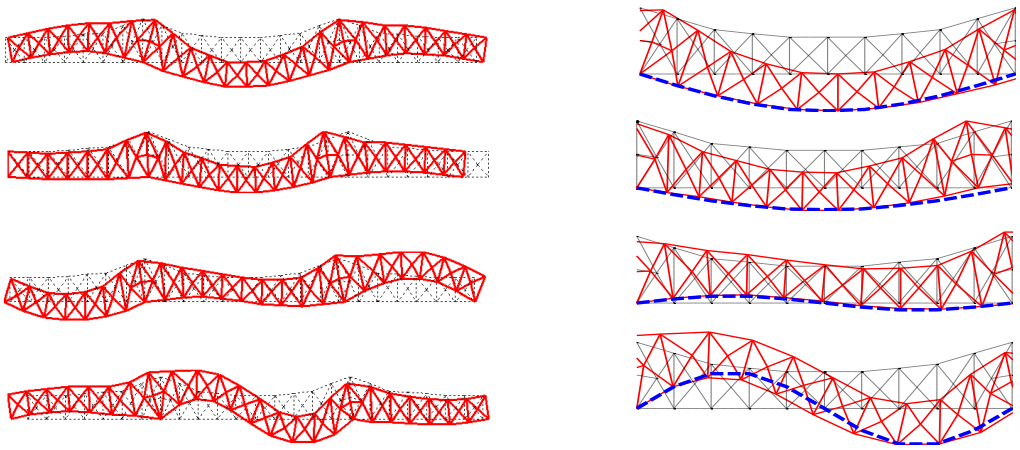

(a) Whole FE model

(b) Second span only: compared with assumed mode shapes

Fig. 11 First four mode shapes of FE model

MATLAB Simulink is used to simulate the displacement, acceleration, and strain of the truss model using a vertical load similar to Fig. 2 moving from left to right on the structure. The acceleration is assumed to be measured at N5, while the strains of the deck are obtained at the mid points of four members between N1-N2, N3-N4, N6-N7, and N8-N9. The simulated acceleration and strains are made contaminated by 5% noise in RMS. Note that acceleration and displacement are obtained in the vertical direction, while the axial strains are obtained on the lower chord members.

Given with 4 strain measurements, the first four mode shapes shown in Fig. 11 are used to build the modal mapping relationship for the strain-based and the improved methods. However, for the acceleration-strain-based method, sinusoidal mode shapes are approximately obtained only for the second span of the continuous truss bridge (Cho *et al*. 2014). Unlike the deck-arch model, the assumed mode shapes are apparently similar to the shapes from the FE model with small discrepancy.

Fig. 12 shows the displacements estimated at N5 by four methods in comparison with the exact ones. The general trends of the results are very similar to those of the deck arch model: the acceleration-based and the strain-based methods show their weakness in pseudo-static and dynamic components of displacement, respectively. Though the acceleration-strain-based method estimates overall shape of the displacement, the amplitude could not be accurately estimated. The improved acceleration-strain-based method estimates the displacement with the best accuracy among the four methods in both low- and high- frequency ranges. The RMSD values of the displacements at N5 are 82.8, 35.1, 34.3, and 22.6% for the four methods, respectively. The error is slightly larger than the deck arch bridge model, but still the proposed improved method gives the smallest error.

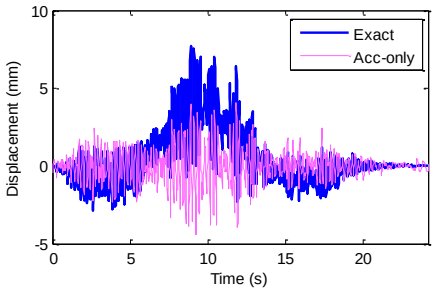

(a) Acceleration-based method

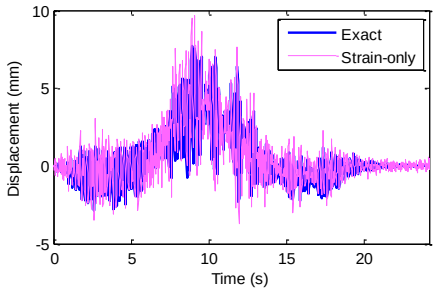

(b) Strain-based method

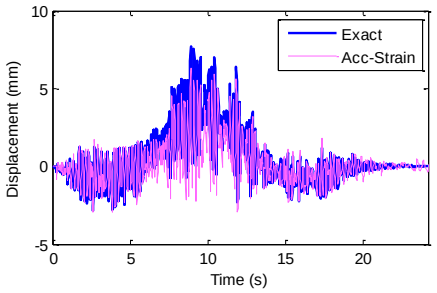

(c) Acceleration-strain-based method

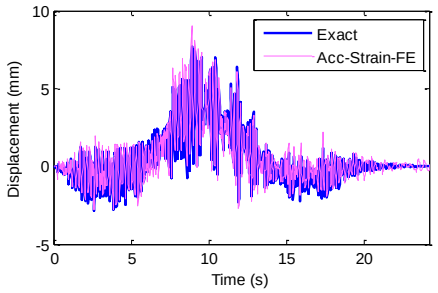

(d) Improved acceleration-strain-based method

Fig. 12 Comparison of displacements estimated at N5 for three-span truss model by four different estimation methods with exact one

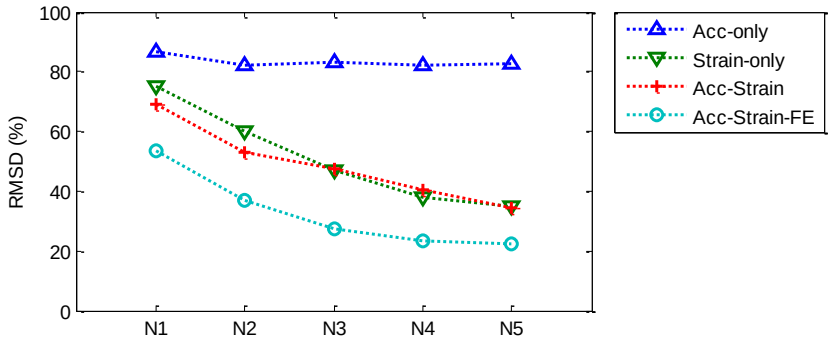

Fig. 13 RMSD of displacements at N1-N5

The RMSD values estimated at 5 locations (N1-N5) by four methods are compared in Fig. 13. Due to the mode shapes assumed similar to the shapes from the FE model (see Fig. 11(b)), the three methods except the acceleration-based method show increasing values as the sensor location gets close to the left support due to smaller amplitude of displacement, while the acceleration-based method shows nearly-constant level of large error due to incorrect estimation of pseudo-static displacements. Similar to the deck arch bridge model, the improved method shows the smallest RMSD values for all locations.

4. Experimental validation

4.1 Test bridge and test setup

To validate the performance of the improved method for a real bridge structure, a field testing was conducted on a prestressed concrete bridge shown in Fig. 14, which was developed as a test-bed of bridge measurement technology by KICT (Korea Institute of Construction Technology). The bridge is a single span prestressed concrete girder bridge with four girders and its span length is 11m.

To estimate the displacement by the improved method, acceleration and strain were measured on the bridge: three strain gages were installed beneath the bridge girder at L1, L3, and L4, and two accelerometers were placed at L2 and L3, as shown in Fig. 14. In addition, two laser displacement sensors were also collocated at L2 and L3 to provide reference displacements. To excite the bridge, a 28.63 ton truck ran on the bridge with the speed of 15 km/h.

4.2 Finite element model of test bridge

To build the modal mapping matrix for the strain-based and the improved methods, an FE model of the bridge was built using ANSYS as shown in Fig. 15. The first three mode shapes for the displacement and strain were extracted from the FE model to build the modal mapping of strain to displacement. Torsional modes have effectively similar shapes to the bending modes for individual girders (Cho *et al*. 2014). Thus, the information of the torsional modes is excluded in the modal mapping procedure.

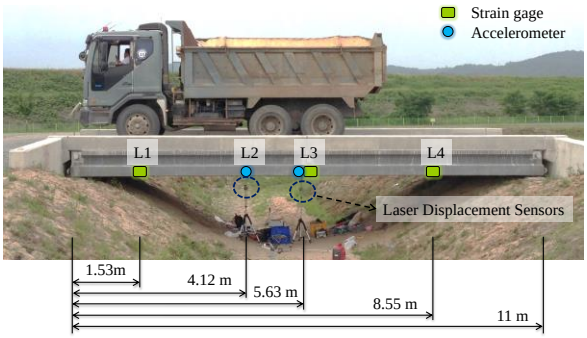

Fig. 14 Test bridge and sensor locations

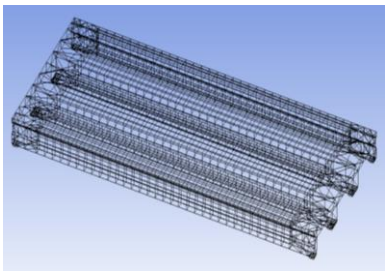

Fig. 15 FE model of test bridge

4.3 Displacement estimation

The displacements at L2 and L3 were estimated by the improved method, and the results were compared with the reference values measured with laser displacement meters. The neutral axis of the bridge was initially assumed to be 0.25 m from the sensor level (bottom of girders) for the strain-based, the acceleration-strain-based, and the improved methods. The neutral axis is compensated in the acceleration-strain-based and the improved methods, but not in the strain-based method. Fig. 16 compares the estimated displacements by four methods with the reference values at L3 when the truck ran. As in the numerical simulations, the acceleration-based method shows weakness in estimating pseudo-static components. The strain-based method cannot estimate accurate pseudo-static component due to the inaccurate neutral axis in the FE model. The acceleration-strain-based and the improved methods estimated displacements very similar to the reference ones as shown in Figs. 16(c) and 16(d).

The RMSD values of the displacements estimated by four methods at L2 and L3 are tabulated in Table 3. While the acceleration-based and the strain-based methods have large errors over 25% in RMSD, the acceleration-strain-based and the improved methods have smaller error. However, the acceleration-strain-based and the improved methods have the smallest measures (less than 6%), since the assumed sinusoidal mode shapes are very good for this beam-type of bridge.

The peak displacement is another important measure for health monitoring of civil infrastructure. Similar to the RMSD, the percentage peak error can be defined as

$$\text{Peak Error } (\%) = \frac{\max u^{est} - \max u^{ref}}{\max u^{ref}} \times 100 \tag{10}$$

The peak errors are calculated and shown in Table 3, which shows that the improved method estimates the peak displacements more accurately than the acceleration-strain-based method: 2.80 and 3.75% versus 3.61 and 6.59% at L2 and L3, respectively. These results indicate that the proposed improved method has better accuracy than the acceleration-strain-based method even for this simply supported bridge. Especially, considering the peak displacement by the moving truck is about 4 mm, the improved method is found to be appropriate for the displacement measurement of civil engineering structures that generally have low displacement levels.

Table 3 RMSD (%) and peak error (%) between estimated and reference displacements

Methods	L2		L3	
	RMSD (%)	Peak Error (%)	RMSD (%)	Peak Error (%)
Acceleration-based method	99.0	-81.4	99.0	-80.3
Strain-based method	28.7	-27.4	33.8	-32.0
Acceleration-strain-based method	5.62	3.61	5.75	6.59
Improved acceleration-strain-based method	5.88	2.80	5.70	3.75

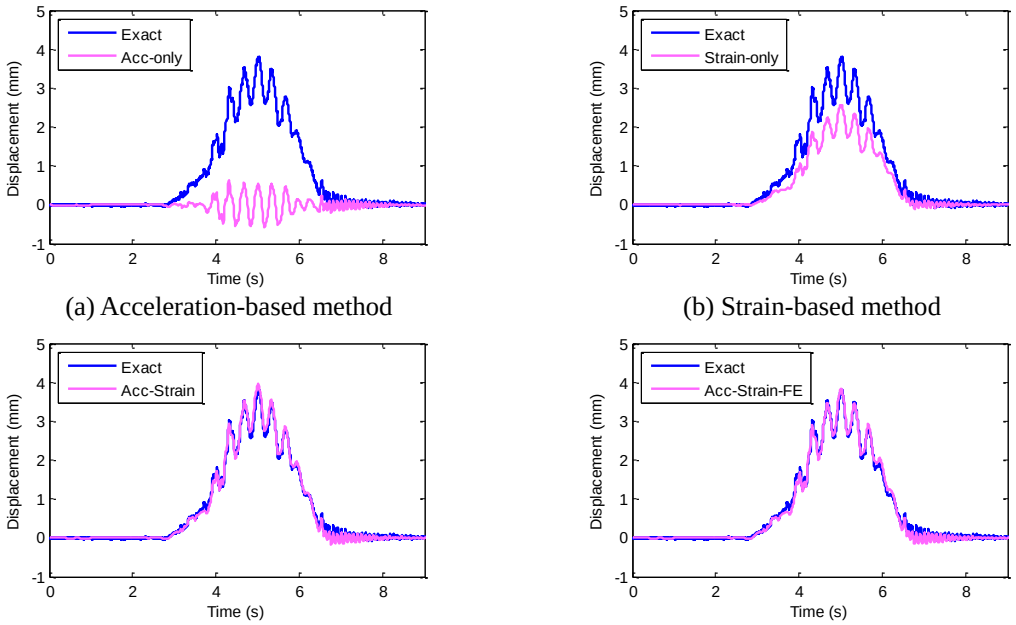

(a) Acceleration-based method (b) Strain-based method

(c) Acceleration-strain-based method (d) Improved acceleration-strain-based method

Fig. 16 Comparison of displacements estimated by improved method with reference: at L3

5. Conclusions

In this paper, an improved displacement estimation method based on data fusion of acceleration and strain has been proposed for the application to general types of bridge structures whose mode shapes may not be assumed in analytical (e.g., sinusoidal) function. The improvement has been made by employing the mode shapes from an FE model in the modal mapping of strain to displacement. The performance of the improved method has been verified by numerical simulations on a deck arch structure and a three-span truss structure with complex shapes. Field experiment on a prestressed concrete bridge has also been carried out. The estimated displacements by four methods, acceleration-based method, strain-based method, acceleration-strain-based method, and improved method, have been compared.

The result of this study can be summarized as:

(1) In the numerical simulations on the deck arch model and the truss model, the proposed method estimated displacements with better accuracy than the other methods at all locations of the structure owing to the accurate modal mapping using the FE model.

(2) The perturbation of the FE model has increased the inaccuracy of the improved method. However, at the center locations, large perturbation (34.6% in RMS) resulted in the RMSD errors of 10.8%, which is less than 20.5% by the acceleration-strain-based method, which shows the effectiveness of the proposed method with somewhat inaccurate FE model.

(3) The proposed method estimated the displacement equivalently well using the strain data on non-beam type members such as truss and arch, which shows its good compatibility of the improved method to more general types of structures.

(4) In the field test on a prestressed concrete bridge, the proposed method accurately estimated the dynamic displacements, whose maximum amplitudes are less than 4mm. The RMSD by the improved method was similar to those by the acceleration-strain-based method, while the peak displacement was estimated more accurately with less than 4% errors.

Acknowledgements

This research was supported by Basic Science Research Program through the National Research Foundation of Korea (NRF) funded by the Ministry of Science, ICT & Future Planning (NRF-2012-R1A1A1-042867). The support is gratefully appreciated.

Reference

Altunisik, A.C., Bayraktar, A. and Ozdemir, H. (2012) "Seismic safety assessment of eynel highway steel bridge using ambient vibration measurements", *Smart Struct. Syst.*, **10**(2), 131-154.

Atkinson, K.E. (2008), *An introduction to numerical analysis*, John Wiley & Sons.

Bani-Hani, K.A., Zibdeh, H.S. and Hamdaoui, K. (2008) "Health monitoring of a historical monument in Jordan based on ambient vibration test", *Smart Struct. Syst.*, **4**(2), 195-208.

Çelibi, M. (2000), "GPS in dynamic monitoring of long-period structures", *Soil Dyn. Earthq. Eng.*, **20**, 477-483.

Cho, S., Sim, S.H., Park, J.W. and Lee, J. (2014), "Extension of indirect displacement estimation method using acceleration and strain to various types of beam structures", *Smart Struct. Syst.*,**14**(4), 699-718.

Chung, W., Kim, S., Kim, N. and Lee, H. (2008), "Deflection estimation of a full scale PSC girder using long-gauge fiber optic sensors", *Constr. Build. Mater.*, **22**(3), 394-401.

Doebling, S.W., Farrar, C.R. and Prime, M.B. (1998), "A summary review of vibration-based damage identification methods", *Shock Vib. Digest*, **30**, 91-105.

Faulkner, B.C., Barton, F., Baber, T.T. and McKeel, W.T. (1996), *Determination of bridge using acceleration data*, Virgina Transportation Research Council. VA, USA.

Foss, G. and Haugse, E. (1995), "Using modal test results to develop strain to displacement transformations", *Proceedings of the 13th Int. Modal Analysis Conf.*

Gindy, M., Nassif, H.H. and Velde, J. (2008), "Bridge displacement estimates from measured acceleration records", *Transport. Res. Rec.*, **2028**, 136-145.

Jo, H., Sim, S.H., Tatkowski, A., Spencer, Jr., B.F. and Nelson, M.E. (2013), "Feasibility of displacement monitoring using low-cost GPS re-ceivers", *Struct. Control Health.*, **20**(9), 1240-1254.

Kandula, V., DeBrunner, L., DeBrunner, V. and Rambo-Roddenberry, M. (2012), "Field testing of indirect displacement estimation using accelerometers", *Proceedings of the Conf. Record of the 46th Asilomar Conf. Signals, Systems, and Computers*.

Kang, L.H., Kim, D.K. and Han, J.H. (2007), "Estimation of dynamic structural displacements using fiber Bragg grating strain sensors", *J. Sound Vib.*, **305**(3), 534-542.

Lee, H.S., Hong, Y.H. and Park, H.W. (2010), "Design of an FIR filter for the displacement reconstruction using measured acceleration in low-frequency dominant structures", *Int. J. Numer. Meth. Eng.*, **82**(4), 403-434.

Lee, J.J., Fukuda, Y., Shinozuka, M., Cho, S. and Yun, C. (2007), "Development and application of a vision-based displacement measurement system for structural health monitoring of civil structures", *Smart Struct. Syst.*, **3**(3), 373-384.

Majumder, M., Gangopadhyay, T.K., Chakraborty, A.K., Dasgupta, K. and Bhattacharya, D.K. (2008), "Fibre Bragg gratings in structural health monitoring—Present status and applications", *Sensor. Actuat.*

A-Phys., **147**(1), 150-164.
Nassif, H.H., Gindy, M. and Davis, J. (2005), "Comparison of laser Doppler vibrometer with contact sensors for monitoring bridge deflection and vibration", *NDT & E Inter.*, **38**, 213-218.
Omenzetter, P., Brownjohn, J.M.W. and Moyo, P. (2004), "Identification of unusual events in multi-channel bridge monitoring data", *Mech. Syst. Signal Pr.*, **18**(2), 409-430.
Park, J.W., Sim, S.H. and Jung, H.J. (2013), "Displacement estimation using multimetric data fusion", *IEEE/ASME Trans. Mechatronics*, **18**(6), DOI: 10.1109/TMECH.2013.2275187.
Park, K.T., Kim, S.H., Park, H.S. and Lee, K.W. (2005), "The determination of bridge displacement using measured acceleration", *Eng. Struct.*, **27**(3), 371-378.
Shin, S., Lee, S.U. and Kim, N.S. (2012), "Estimation of bridge displacement responses using FBG sensors and theoretical mode shapes", *Struct. Eng. Mech.*, **42**(2), 229-245.
Sigurdardottir, D.H. and Glisic, B. (2014), "Detecting minute damage in beam-like structures using the neutral axis location", *Smart Mater. Struct.*, **23**(12), 125042.
Xu, L., Guo, J.J. and Jiang, J.J. (2002), "Time-frequency analysis of a suspension bridge based on GPS", *J. Sound Vib.*, **254**(1), 105-116.